g factors of first 2⁺ states of neutron-rich Xe, Ba, and Ce isotopes

C. Goodin,[1] J. R. Stone,[2,3,4] N. J. Stone,[2,4] A. V. Ramayya,[1] A. V. Daniel,[1,5] J. H. Hamilton,[1] K. Li,[1]
J. K. Hwang,[1] G. M. Ter-Akopian,[5] and J. O. Rasmussen[6]

[1]*Physics Department, Vanderbilt University, Nashville, Tennessee 37235, USA*
[2]*Department of Physics, Oxford University, Oxford OX1 3PU, United Kingdom*
[3]*Department of Chemistry and Biochemistry, University of Maryland, College Park, Maryland 20742, USA*
[4]*Department of Physics and Astronomy, University of Tennessee, Knoxville, Tennessee 37996, USA*
[5]*Flerov Laboratory of Nuclear Reactions, JINR, Dubna, Russia*
[6]*Lawrence Berkeley National Laboratory, Berkeley, California 94720, USA*

Using new techniques developed for measuring angular correlations with large detector arrays, the *g* factors of 2⁺ states in ^{140,142}Xe are measured for the first time by the method of correlation attenuation in randomly oriented magnetic fields. *g* factors in ^{146}Ba and ^{146,148}Ce are measured to establish the method by comparison with previous values. The results are discussed in terms of IBM-2 and rotation-vibration models.

I. INTRODUCTION

Nuclear *g* factors give insight into the collective and single-particle structure of nuclear states. It is valuable to measure *g* factors for isotopic chains to observe the behavior moving away from closed shells. Systematic trends in *g* factors of 2_1^+ states or higher yrast states can indicate the presence of subshell closures or other structure changes. In this work, the systematics of *g* factors in neutron-rich, even-even Xe isotopes have been extended. The *g* factors of 2_1^+ states in ^{146}Ba and ^{146,148}Ce have been measured and are compared to those of previous work.

The Xe nuclei with $Z = 54$ and $N = 86$ (88) with two proton pairs above the $Z = 50$ shell closure and two (three) neutron pairs above the $N = 82$ shell closure are transitional between spherical and deformed shapes. Assuming vibrational collectivity is dominant for low-energy excitations in ^{140,142}Xe, *g* factors in these nuclei are compared with predictions of the IBM-2. Because ^{146}Ba and ^{146,148}Ce show moderate axial quadrupole deformation with $\beta_2 \sim 0.2$ [1], both the IBM-2 and rotation-vibration model with independent proton and neutron deformations [2] are considered in discussion of the results for these nuclei.

The measurements in this work on nuclei (^{140,142}Xe) with only a few proton and neutron bosons above ^{132}Sn provide a test of the accepted parametrization of the boson *g* factors in the IBM-2. The result of a fit to the *g*-factor measurements from this work and other recent and past measurements is discussed.

II. EXPERIMENT AND DATA ANALYSIS

The data for this analysis were taken by using the Gammasphere detector array located at Lawrence Berkeley National Laboratory. A ^{252}Cf spontaneous fission source with an α activity of 62 μCi was placed between two iron foils. The foils were in place to stop the fission fragments, eliminating the need for a Doppler correction. Approximately 4×10^{11} triple- and higher-fold γ coincidence events were recorded. More details about this experiment can be found in Luo *et al.* [3].

In this work, the angular resolution of Gammasphere, which has 64 unique angles between detector pairs, is used to perform *g*-factor measurements through perturbed angular correlations. Because of the extremely high statistics of this data set, coincidences can be cleanly selected by applying additional gates to the correlation of interest. For example, when the correlation of a given $4^+ \rightarrow 2^+ \rightarrow 0^+$ cascade is measured, only events in coincidence with the $6^+ \rightarrow 4^+$ or the $8^+ \rightarrow 6^+$ transitions have been used in suitable cases. Fig. 1 illustrates the preparation of the data for ^{140}Xe. The left part of the figure shows simple two-fold coincidences as a function of the two photon energies. The right part shows the significant suppression of random background achieved by applying the additional gates listed in Table I.

III. THE IPAC TECHNIQUE FOR *g*-FACTOR MEASUREMENT

As mentioned, the fission fragments were stopped in iron foils and were therefore subject to the magnetic hyperfine fields (B_{HF}) in the iron lattice caused by their implantation in substitutional sites. For a nuclear state with lifetime τ, the spin vector of the nucleus will rotate about B_{HF} over the lifetime of the state, with the frequency of the rotation proportional to the strength of the field and the *g* factor of the state. For this experiment, the magnetic domains in the iron foils remained randomly aligned; the foils were not cooled and there was no applied external field. The net result of the rotation of the implanted nuclei about the randomly oriented fields is an attenuation of the expected angular correlation. This is the basis of the integral perturbed angular correlation technique (IPAC) for *g*-factor measurement. The attenuation factor G_k is related to the Larmor precession frequency ω_L and the lifetime τ by [4]:

$$G_k = \frac{1}{2k+1}\left(1 + 2\sum_{q>0}^{k}\frac{1}{1+q^2\phi^2}\right) \qquad (1)$$

$$\phi = \omega_L\tau. \qquad (2)$$

TABLE I. Parameters and experimental angular correlation coefficients used in the g-factor calculations. The additional gates are either coincident transitions in the isotope of interest or transitions in partner nuclei. For example, for ^{142}Xe, the 242-keV transition is from the fission partner ^{108}Ru. No error is quoted for the A_4 value for ^{136}Xe because the parameter was held fixed at the asymptote. Hyperfine fields are discussed in the text.

Nucleus	τ (ns)	B_{HF} (T)	A_2^{exp}	A_4^{exp}	Additional gates (keV)
^{136}Xe	1.87(25)		0.023(3)	0.001	None
^{140}Xe	0.163(7)	73(8)	0.095(4)	0.010(6)	583,566,607,738,242,423,575,937
^{142}Xe	0.49(14)	73(8)	0.079(9)	0.001(14)	242,270,490,551
^{144}Ba	1.02(3)		0.066(4)	0.008(6)	431,509
^{146}Ba	1.24(4)	37(6)	0.068(8)	0.010(11)	445,524,511,569
^{146}Ce	0.36(4)	41(2)	0.086(4)	0.011(7)	503,565,515,380
^{148}Ce	1.45(9)	41(2)	0.046(6)	0.001(9)	386,451,501,537

Experimentally, the attenuation factors $G_{2,4}$ are defined by fitting the measured angular correlation to the parameters A_2^{exp} and A_4^{exp}

$$W(\theta) = A_0\left[1 + A_2^{exp} P_2(\cos\theta) + A_4^{exp} P_4(\cos\theta)\right] \quad (3)$$

$$G_k = \frac{A_k^{exp}}{A_k^{theory}}. \quad (4)$$

The A_0 coefficient is for normalization only. For pure (unmixed) transitions, the $A_{2,4}^{theory}$ can be calculated with the Wigner 3-j and 6-j coefficients, as outlined and tabulated by Taylor *et al.* [5]. With these theoretical values, the attenuation of angular correlations can be used to calculate the g factor

using Eq. (4) and

$$g = -\frac{\hbar\phi}{\mu_N B_{HF}\tau}. \quad (5)$$

An example of an unattenuated angular correlation is shown in Fig. 2, which is the correlation for the $4^+ \rightarrow 2^+ \rightarrow 0^+$ cascade in ^{142}Ba. For this correlation (as for all correlations in this work) $A_2^{theory} = 0.102$, $A_4^{theory} = 0.0089$. Figure 3 shows an example of an attenuated correlation for ^{142}Xe. It is important to note that ϕ, which is proportional to the product $g B_{HF}\tau$, must fall within certain limits for this method to be applicable. If ϕ is very small, the correlation is unattenuated and if ϕ is large, then the G_k values approach their asymptotic limits of $G_2^{\phi\rightarrow\infty} = \frac{1}{5}$ and $G_4^{\phi\rightarrow\infty} = \frac{1}{9}$, giving no useful information. In iron, hyperfine fields are of the order
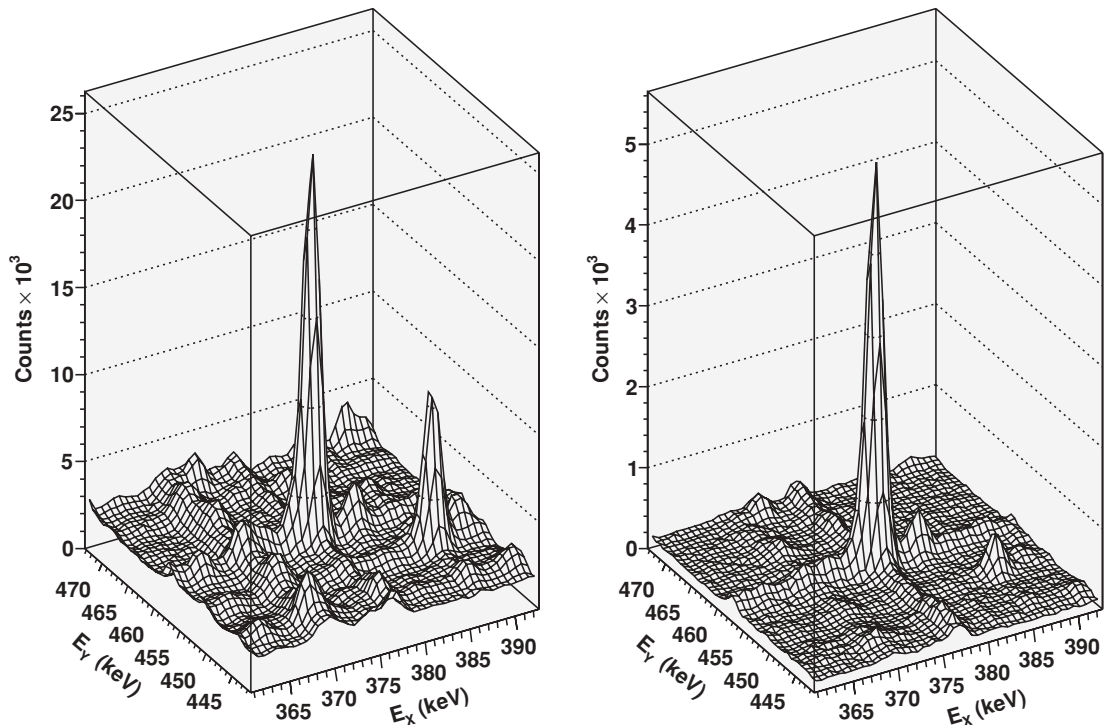

FIG. 1. Two-dimensional coincidences for the $\cos(\theta) = 0$ angle of Gammasphere for $4^+ \rightarrow 2^+ \rightarrow 0^+$ cascade in ^{140}Xe. For details see text.
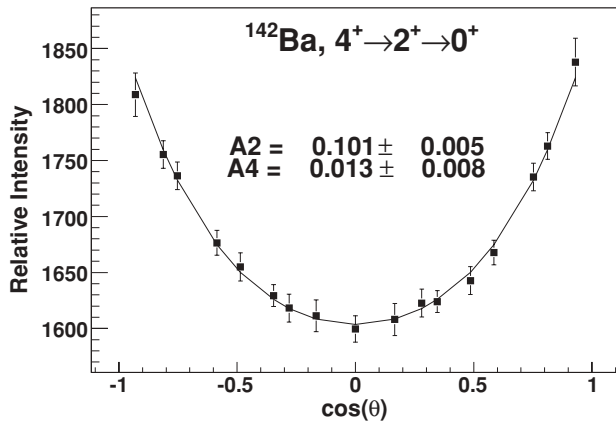
FIG. 2. Example of an unattenuated angular correlation in ^{142}Ba. The correlation is unattenuated because the lifetime of the 2_1^+ state is only 0.12 ns and B_{HF} is relatively low, 37(6) T.

10–100 T and it follows that typical g factors for states with lifetimes of roughly a nanosecond can be measured by IPAC with the source/foil arrangement used here.

To extract the nuclear g factor from the attenuation measurement, the hyperfine field must be known. It was shown in our previous article on this method [6] that the hyperfine fields are not aligned and that no electric fields are created due to radiation damage in the foil. The compilation by G. N. Rao [7] is a useful, if somewhat outdated, source for B_{HF} values. Those adopted in this work are discussed below.

Although the general aspects of this method are outlined here, there are many details associated with the solid angle correction, binning of the data, and relative detector efficiencies. These details can be found in Ref. [6]. As a final note, it is clear from Eq. (1) that this method can measure only the magnitude, and not the sign, of the g factor. However, both systematics and theory give a good indication that the nuclei measured in this work should have positive g factors.

IV. RESULTS

The results of the angular correlations in this work are summarized in Table I, which also gives the hyperfine fields

FIG. 4. Attenuated angular correlation for the $4^+ \rightarrow 2^+ \rightarrow 0^+$ cascade in ^{146}Ba.

and state lifetimes used to calculate the g factors. All the lifetimes are taken from the National Nuclear Data Center [8] compilations.

The $4^+ \rightarrow 2^+ \rightarrow 0^+$ correlation for ^{142}Xe is shown in Fig. 3. As a check on the value of the hyperfine field, the correlation through the 4^+ state in ^{136}Xe was measured and the hyperfine field was calculated by using the g factor $g(4_1^+) = 0.80(15)$ [9]. The result, $B_{HF}(\text{Xe}) = 87(30)$ T, is consistent with the value $B_{HF}(\text{Xe}) = 73(8)$ T given in Ref. [7]. Adopting the latter value, the ^{140,142}Xe 2_1^+ g factors are found to be 0.35(12) and 0.25(10), respectively.

The $4^+ \rightarrow 2^+ \rightarrow 0^+$ correlation for ^{146}Ba is shown in Fig. 4. The g factor of the 2_1^+ state in ^{146}Ba is found to be 0.27(10). For this measurement, the hyperfine field was calibrated using the observed attenuation in ^{144}Ba with the known g factor $g(2_1^+) = 0.34(5)$ [10], which gave the value $B_{HF}(\text{Ba}) = 37(6)$ T. Although this value is much larger than that tabulated in Ref. [7], the tabulated value leads to a physically unreasonable result, so the calibrated value is adopted for this work.

The $4^+ \rightarrow 2^+ \rightarrow 0^+$ correlation for ^{146}Ce is shown in Fig. 5. The g factors of the 2_1^+ states in ^{146,148}Ce were found to be 0.46(10) and 0.39(8), respectively, taking the hyperfine
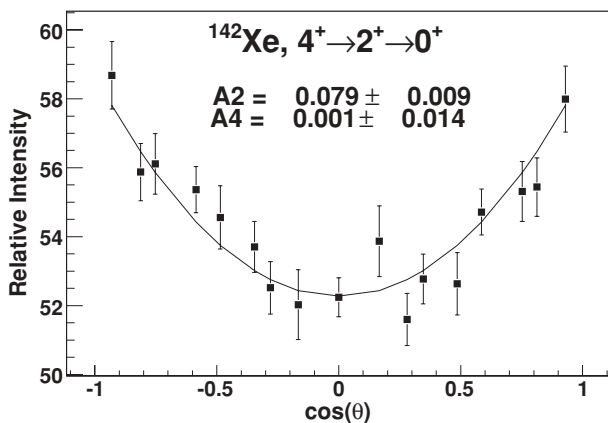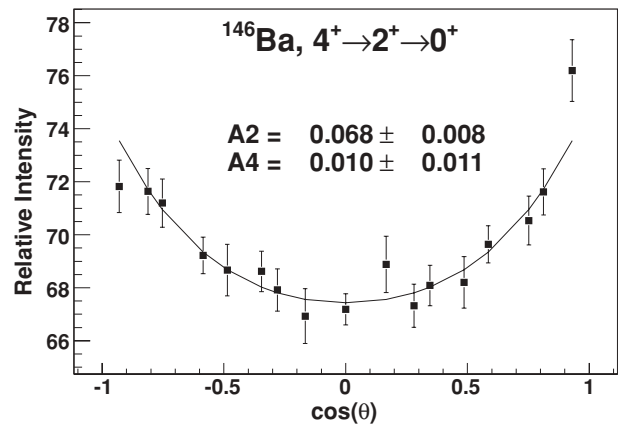

FIG. 3. Attenuated angular correlation for the $4^+ \rightarrow 2^+ \rightarrow 0^+$ cascade in ^{142}Xe.
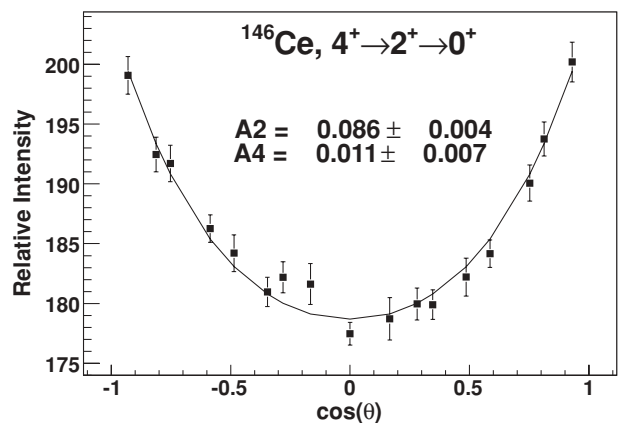

FIG. 5. Attenuated angular correlation for the $4^+ \rightarrow 2^+ \rightarrow 0^+$ cascade in ^{146}Ce.

TABLE II. *g* factors of 2_1^+ states measured in this work, calculated using the parameters in table I.

Nucleus	g	Previous measurements
^{140}Xe	0.35(12)	
^{142}Xe	0.25(10)	
^{146}Ba	0.27(9)	0.28(7) [10], 0.20(10) [11]
^{146}Ce	0.46(10)	0.24(5) [12], 0.46(34) [11]
^{148}Ce	0.39(8)	0.37(6) [12]

field to be 41(2) T [7]. The *g* factor for ^{146}Ce differs from our previously published value [6] because more restrictive gating conditions were used for the measurement in this work, giving cleaner spectra.

The results of all measurements are shown in Table II, where they are compared with any previous measurements. The errors quoted include contributions from the attenuation measurement, lifetime, and hyperfine fields. The results are compared with theory in the following section.

V. DISCUSSION

In the simplest macroscopic model the g_R factor of a deformed even-even nucleus is obtained assuming protons and neutrons to have equal axial deformation and respective orbital *g* factors of 1 and 0, with the result $g_R = Z/A$. Greiner [2] extended this model by considering different proton and neutron axial deformations having ratio $R = \beta_2(n)/\beta_2(p)$ with the result for g_R of the ground-state rotational band

$$g_R = \frac{Z}{A} \times (1 - 2f), \qquad (6)$$

where f is

$$f \approx \frac{N}{A}(R - 1). \qquad (7)$$

For $R > 1$, neutrons carry the greater proportion of the angular momentum and the *g* factor falls below Z/A and vice versa. In Greiner's work, R was taken to be solely determined by proton(neutron) pairing strengths $G_p(G_n)$

$$\frac{1}{R} = \frac{\beta_2(p)}{\beta_2(n)} = \sqrt{\frac{G_n}{G_p}}. \qquad (8)$$

Values $G_n = 18/A$ MeV and $G_p = 25/A$ MeV [13] and $G_n = 20/A$ MeV and $G_p = 30/A$ MeV [14] were suggested, making the ratio R a constant of the model with a value close to 1.2. These relations are close to more recent estimates for the proton and neutron pairing strengths ([15,16]).

For vibrational nuclei, Eq. (6) takes the form

$$g_v \approx \frac{Z}{A} \times \left(1 - \frac{4}{3}f\right) \qquad (9)$$

with the same definition of f as above. Quantities $\beta_2(p)$ and $\beta_2(n)$ in vibrational nuclei are understood as "effective" deformations.

An alternative interpretation of the *g* factor of a collective 2^+ state is given by the IBM-2 [17], which predicts

$$g_{2^+} = g_\pi \frac{N_\pi}{N} + g_\nu \frac{N_\nu}{N}, \qquad (10)$$

where $N_{\pi(\nu)}$ is the number of proton (neutron) bosons or boson holes outside the nearest closed shell and $N = N_\pi + N_\nu$. The parameters g_π and g_ν are the effective proton and neutron boson *g* factors, respectively. Microscopic calculations yield $g_\pi = 1$ and $g_\nu = 0$. However, an analysis by Wolf *et al.* [18] of *g* factors of neutron-rich Ce, Nd, and Sm isotopes indicated that effective boson *g* factors of $g_\pi = 0.63(4)$ and $g_\nu = 0.05(5)$ better describe the nuclei in this region. A later analysis by Gill *et al.* [12] for heavy Ba isotopes confirmed this choice of parameters.

In this work, the proton and neutron effective *g* factors were extracted from an updated version of the calibration from Ref. [18] that includes 2_1^+ *g* factors taken from both a recent compilation [19] and the measurements in this article. In this fit, Eq. (10) is multiplied by N/N_ν, and the values of g_π and g_ν are then given by a linear fit to N_π/N_ν vs. gN/N_ν. The fit, shown in Fig. 6, yields the effective *g* factors $g_\pi = 0.67(6)$, $g_\nu = 0.02(7)$. The data used in this fit are given in Table III. Although these results are consistent with those of Ref. [18], they are somewhat closer to the theoretical estimates. Two things should be noticed. First, the results of this work can be seen to be consistent (within somewhat large errors) with the IBA2 model prediction of a linear dependence of $g(2^+)N_\pi/N_\nu$ on N_π/N_ν. Second, the large errors in the new data mean that they do not significantly affect the fit values of g_π and g_ν. The new calibration presented here is given for use in interpretation of future *g* factor measurments. Keeping

TABLE III. Experimental *g* factors of 2_1^+ states above ^{132}Sn found in this and previous work.

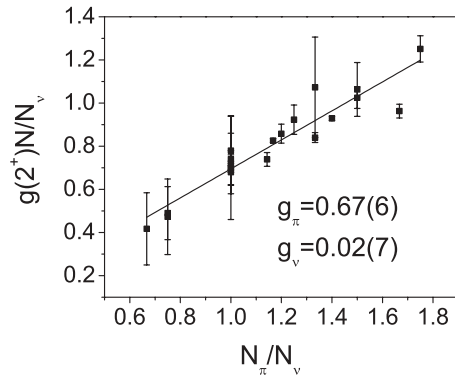| Nucleus	N_π/N_ν	g_{exp}	Reference
^{140}Xe	1	0.35(12)	This work
^{142}Xe	0.667	0.25(10)	This work
^{142}Ba	1.5	0.425(50)	[19]
^{144}Ba	1	0.34(5)	[19]
^{146}Ba	0.75	0.27(10)	This work
^{146}Ba	0.75	0.28(7)	[19]
^{146}Ce	1.333	0.46(10)	This work
^{148}Ce	1	0.39(8)	This work
^{148}Ce	1	0.37(6)	[12]
^{148}Nd	1.667	0.361(12)	[19] (average)
^{150}Nd	1.25	0.41(3)	[19] (average)
^{152}Sm	1.5	0.41(2)	[19] (average)
^{154}Sm	1.2	0.39(2)	[18]
^{154}Gd	1.75	0.455(22)	[19] (average)
^{156}Gd	1.4	0.387(4)	[19]
^{158}Gd	1.167	0.381(4)	[19]
^{160}Gd	1	0.36(2)	[19]
^{160}Dy	1.333	0.36(1)	[19] (average)
^{162}Dy	1.143	0.345(15)	[19]
^{164}Dy	1	0.35(1)	[19] (average)

FIG. 6. Linear least-squares fit of the IBM-2 parameters to experimentally measured 2$^+$ states in nuclei above ^{132}Sn. In this fit, the slope is given by g_π and the intercept by g_ν.

this in mind, this calibration is used in Figs. 7–9 for display purposes.

The measurement of *g* factors in ^{140,142}Xe extends the knowledge of systematics for Xe isotopes above ^{132}Sn. Although the Ba and Ce isotopes considered here are at least moderately deformed, the Xe isotopes are relatively closer to shell closure at ^{132}Sn, and *g* factor calculations based on microscopic single-particle theory should also be considered. Brown *et al.* [20] calculated magnetic moments of 2$_1^+$ states in lighter $^{134-138}$Xe using the shell model with a residual interaction based on the CD-Bonn renormalized *G* matrix, and results of these calculations are shown for completeness in this work.

Speidel *et al.* [21] have measured *g* factors of 2$_1^+$ states in ^{134,136}Xe, and Jakob *et al.* [22] in ^{130,132,134,136}Xe. The results are shown in Fig. 7, along with the present measurements for ^{140,142}Xe. The figure reveals almost perfect symmetry about $N = 82$ as a function of neutron number, suggesting very similar makeup of the first 2$^+$ states below and above the shell closure and symmetry between neutron-hole and
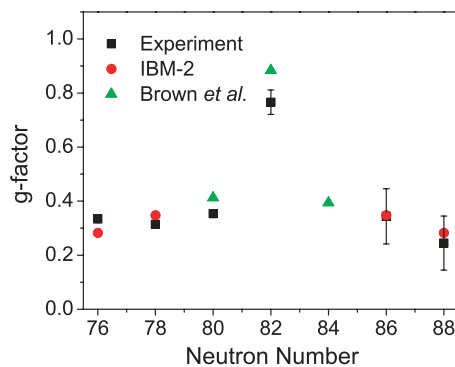

FIG. 8. (Color online) The *g* factors of the 2$_1^+$ states in barium isotopes near the $N = 82$ shell closure. The black squares are experimental data, the red circles are the prediction of the IBM-2 using the parameters from the fit discussed in the text, and the green triangles are from the calculation by Brown *et al.* [20]. The point for $N = 90$ ^{148}Ba is from this work, while the points below $N = 82$ are from Brennan *et al.* [23]. The $N = 82$ point is from Bazzacco *et al.* [25], $N = 86$ is from Wolf *et al.* [10], and $N = 88$ is from Smith *et al.* [11].

neutron-particle excitations. Both shell-model [20] and the IBM-2 predictions, also shown in the figure, support this conclusion. The agreement with the IBM-2 model suggests the presence of vibrational collectivity (there is no appreciable axial deformation) in ^{130,132,140,142}Xe 2$_1^+$ states. There is also a possibility that the 2$_1^+$ states in ^{130,132,140,142}Xe have still significant single-particle component as the *g* factors seem to follow smoothly the trend predicted by the shell model when going away from the shell closure. Unfortunately, the extension of the microscopic model further beyond the shell closure is not feasible at the present time.

The 2$_1^+$ state in ^{146}Ba is measured here for comparison and validation of the experimental method. The result, $g(2_1^+) = 0.27(9)$ is in good agreement with both Refs. [11] and [10], who found $g(2_1^+) = 0.20(10)$ and $0.28(7)$, respectively. Lighter

FIG. 7. (Color online) The *g* factors of the 2$_1^+$ states in xenon isotopes near the $N = 82$ shell closure. The black squares are experimental data, the red circles are the prediction of the IBM-2 using the parameters from the fit discussed in the text, and the green triangles are from the calculation by Brown *et al.* [20]. The data for ^{140,142}Xe are from this work, the other data from Jakob *et al.* [22].
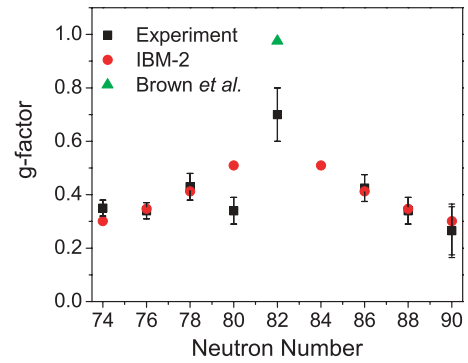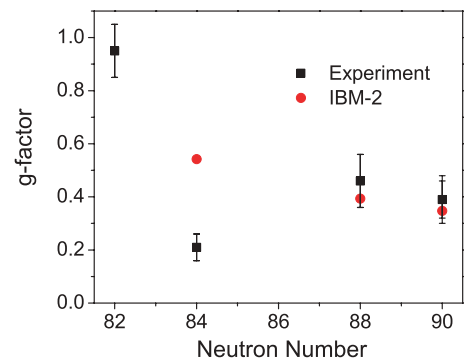

FIG. 9. (Color online) The *g* factors of the 2$_1^+$ states in cerium isotopes near the $N = 82$ shell closure. The black squares are experimental data, the red circles are the prediction of the IBM-2 using the parameters from the fit discussed in the text. The data for $N = 82, 84$ are from Bazzacco *et al.* [28], whereas the data for $N = 88, 90$ are from this work.

TABLE IV. Experimental and calculated values of R, the ratio of neutron to proton deformation. For detail see text.

Nucleus	g_{exp}	R_{exp}	R(SLy4)	R(SkI3)
^{146}Ba	0.27(9)	1.24(20)	1.01	1.02
^{146}Ce	0.46(10)	0.87(21)	0.95	0.95
^{148}Ce	0.39(8)	1.00(16)	0.98	1.00

isotopes ^{130,132,134,136}Ba were measured by Brennan *et al.* [23], and ^{134}Ba was earlier measured by Eberhardt *et al.* [24].

The experimental and theoretical g factors for the first 2^+ state in $^{130-146}$Ba are shown in Fig. 8. Figure 8 also shows the predictions of the IBM-2 using the effective boson g factors determined in this work, as well as the result of the calculation by Brown *et al.* [20]. The remarkable symmetry of the xenon isotopes with respect to $N = 82$ is still present for these barium isotopes, with a possible indication of a lower g factor at $N = 90$. Again, we attribute the good agreement between IBM-2 results and the experiment to presence of vibrational collectivity closer to the shell closure.

The 2^+_1 states in ^{146,148}Ce are also measured here to be compared with previous results on ^{146,148}Ce [12] and ^{146}Ce [11]. The results of all measurements are given in Table II. Agreement of our result with that of Gill *et al.* [12] for ^{148}Ce is good. However, for ^{146}Ce, although the result of Smith *et al.* [11] is consistent with our more precise value, there is strong disagreement with Gill *et al.* [12], who report a striking difference between the two isotopes that our results do not confirm. Comparison of experimental g factors and results of IBA2 calculation for cerium isotopes is shown in Fig. 9.

Development of axially symmetric deformation in ^{146}Ba and ^{146,148}Ce offers an opportunity to explore the properties of the ground states of these nuclei in the framework of the rotational-vibrational model. As stated above, the only variable parameter of this model, the ratio R of the neutron and proton deformations, was assumed to be a constant, related only to the pairing strengths between protons and between neutrons. More recently, mean-field microscopic models predict differences between proton and neutron deformation having a more complex origin and of ratios differing with mass number. Experimental g factors of the 2^+_1 states in deformed nuclei offer a way to deduce R from experiment and test the original model hypothesis. Equations (6) and (7) can be rewritten as

$$R = \frac{A}{N}f + 1,\tag{11}$$

where

$$f = 0.5\left(1 - \frac{A}{Z}g\right).\tag{12}$$

and the experimental values of R compared with the results of an independent microscopic calculation of neutron and proton axial deformation parameters. Mean-field Hartree-Fock+BCS calculation with two Skyrme interactions, SLy4 [26] and SkI3 [27], have been performed for this purpose as part of this work. The results, shown in Table IV, indicate theoretical values of R close to unity in this region, in good agreement with experiment, although lower than the value of 1.2 expected if

the proton and neutron deformation were dependent only on the strength of the proton and neutron pairing forces. This finding supports a more complex origin of proton and neutron density distribution in deformed even-even nuclei. Despite the somewhat large errors in the presently available g factors, this analysis demonstrates the potential ability to extract important information on the relative distribution of proton and neutron densities from sufficiently accurate 2^+_1 g factors within this model.

A similar analysis can be applied to ^{140,142}Xe under the assumption that the 2^+_1 states have a vibrational character. Applying Eqs. (7) and (9) yields $R_{exp} = 1.13(45)$ and $R_{exp} = 1.46(35)$ for ^{140}Xe and ^{142}Xe, respectively. Microscopic calculations of "effective" proton and neutron deformations in even-even vibrational nuclei are not available at present.

VI. CONCLUSION

In this work the g factors of the first 2^+ states in ^{140,142}Xe, ^{146}Ba, and ^{146,148}Ce found by using new techniques developed for measuring angular correlations with large detector arrays are reported. The g factors of 2^+_1 states in ^{140,142}Xe are measured for the first time, whereas the g factors in ^{146}Ba and ^{146,148}Ce are found to have good overall agreement with previously measured values, thus confirming the reliability of the experiment and analysis. The experimental results compare well with the predictions of the IBM-2, suggesting the presence of vibrational collectivity in the 2^+_1 states in question, although single-particle components in the wave functions cannot be excluded. Using measured values of ^{146}Ba and ^{146,148}Ce, a method is outlined that potentially yields information on the ratio of neutron to proton deformation in deformed nuclei. The ratios obtained, although not very precise, are in sensible agreement with results of microscopic calculation using the HF+BCS model with a Skyrme interaction in these less deformed nuclei. If the experimental errors in g factors could be reduced in the future, this information would provide a valuable challenge to models of deformed even-even nuclei.

[1] P. Möller, J. R. Nix, W. D. Myers, and W. J. Swiatecki, At. Data Nucl. Data Tables **59**, 185 (1995).

[2] W. Greiner, Nucl. Phys. **80**, 417 (1966).

[3] Y. Luo *et al.*, Phys. Rev. C **64**, 054306 (2001).

[4] E. Matthias, S. S. Rosenblum, and D. A. Shirley, Phys. Rev. Lett. **14**, 46 (1965).

[5] H. W. Taylor, B. Singh, F. S. Prato, and R. McPherson, Nucl. Data Tables A **9**, 1 (1971).

[6] A. V. Daniel *et al.*, Nucl. Instrum. Methods B **262**, 399 (2007).

[7] G. N. Rao, Hyperfine Interact. **26**, 1119 (1985).

[8] NNDC, http://www.nndc.bnl.gov/bricc/.

[9] Z. Berant *et al.*, Phys. Rev. C **31**, 570 (1985).

[10] A. Wolf, R. L. Gill, H. Mach, R. F. Casten, and J. A. Winger, Phys. Rev. C **37**, 1253 (1988).

[11] A. G. Smith *et al.*, AIP Conf. Proc. **481**, 283 (1999).

[12] R. L. Gill *et al.*, Phys. Rev. C **33**, 1030 (1986).

[13] S. G. Nilsson and O. Prior, Mat. Fys. Medd. Dan. Vid. Selsk. **32**, 16 (1961).

[14] E. R. Marshalek and J. O. Rasmussen, Nucl. Phys. **43**, 438 (1963).

[15] S. Nilsson *et al.*, Nucl. Phys. **A131**, 1 (1969).

[16] I. Ragnarsson and R. Sheline, Phys. Scr. **29**, 385 (1984).

[17] A. Arima, T. Ohtsuka, F. Iachello, and I. Talmi, Phys. Lett. **B66**, 205 (1977).

[18] A. Wolf, D. Warner, and N. Benczer-Koller, Phys. Lett. **B158**, 7 (1985).

[19] N. J. Stone, At. Data Nucl. Data Tables **90**, 75 (2005).

[20] B. Brown *et al.*, Phys. Rev. C **71**, 044317 (2005).

[21] K. H. Speidel *et al.*, Nucl. Phys. **A552**, 140 (1993).

[22] G. Jakob *et al.*, Phys. Rev. C **65**, 024316 (2002).

[23] J. M. Brennan, M. Hass, N. K. B. Shu, and N. Benczer-Koller, Phys. Rev. C **21**, 574 (1980).

[24] J. Eberhardt and K. Dybdal, Hyperfine Interact. **7**, 387 (1979).

[25] D. Bazzacco *et al.*, Z. Phys. A **328**, 275 (1987).

[26] E. Chabanat *et al.*, Nucl. Phys. **A635**, 231 (1998).

[27] P. Reinhard and H. Flocard, Nucl. Phys. **A584**, 467 (1995).

[28] D. Bazzacco *et al.*, Nucl. Phys. **A533**, 541 (1991).